

Development of a powered mobile module for the ArmAssist home-based telerehabilitation platform

Je Hyung Jung, David B. Valencia, Cristina Rodríguez-de-Pablo, Thierry Keller, and Joel C. Perry

Rehabilitation Area, Health Division
TECNALIA

Mikeletegi Pasealekua 1-3, E-20009, Donostia-San Sebastian, Spain

{[jehyung.jung](mailto:jehyung.jung@tecnalia.com), [david.valencia](mailto:david.valencia@tecnalia.com), [cristina.rodriguez](mailto:cristina.rodriguez@tecnalia.com), [thierry.keller](mailto:thierry.keller@tecnalia.com), [joel.perry](mailto:joel.perry@tecnalia.com)}@tecnalia.com

Abstract— The ArmAssist, developed by Tecnia, is a system for at-home telerehabilitation of post-stroke arm impairments. It consists of a wireless mobile base module, a global position and orientation detection mat, a PC with display monitor, and a tele-rehabilitation software platform. This paper presents the recent development results on the mobile module augmenting its functionality by adding actuation components. Three DC servo motors were employed to drive the mobile module and a position control algorithm based on the kinematic model and velocity mode control was implemented such that the module tracks a path defined in the training software. Pilot tests of the powered mobile module were performed in experiments with different load conditions and two unimpaired subjects. Both test results show that the module is able to follow the pre-defined path within an acceptable error range for reach movement training. Further study and testing of the system in realistic conditions following stroke will be a future topic of research.

Keywords—*ArmAssist; arm rehabilitation; stroke rehabilitation; training at home; telerehabilitation*

I. INTRODUCTION

Over the past couple of decades, robotic technology has rapidly drawn clinical attention as the technology that enables more efficient and systematic therapy for rehabilitation following neurologic injuries such as stroke and spinal cord injury. As a result, many robotic systems for upper and lower limb rehabilitation have been developed and tested in academic and clinical settings while some of them have already been commercialized, as presented in [1] and references therein. Moreover, several published research works on the utility of robot-mediated therapy have suggested that the use of a robot in the field of rehabilitation could be a solution to the high level of energy and time that conventional therapy demands of therapists, as well as to the high cost that it demands of patients.

For reasons of size and cost, most robotic systems developed until now have been intended for patients in the sub-acute phase of stroke during their stay at large rehabilitation centers or hospitals. The size and cost limitations prevent patients from receiving adequate continuity of training after discharge, resulting in the shorter training duration and slower recovery speeds than those that could be achieved with lower cost, portable technologies. Hence, it is believed that solutions

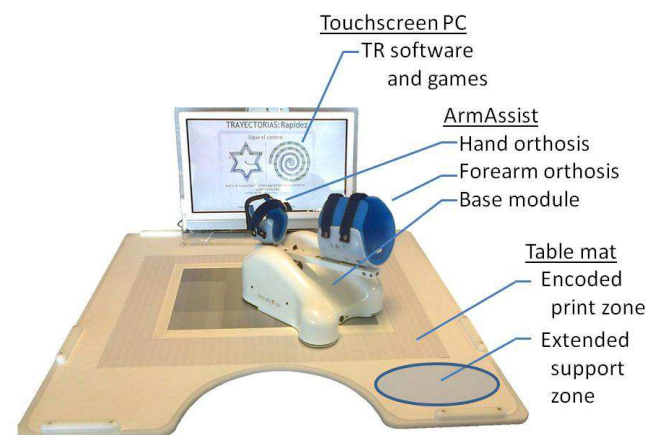


Figure 1. Components of the ArmAssist system for at-home telerehabilitation of post-stroke arm deficits.

bridging this gap are inevitable in order to take advantage of the known benefits of longer duration and higher intensity training spanning the clinical-to-home transfer. This belief was one of the prime motivators behind the development of a portable low-cost platform named the ArmAssist for at-home telerehabilitation of post-stroke arm impairments [1].

The previous (non-motorized) ArmAssist system (Fig. 1) consists of a wireless mobile base module, a global position and orientation detection mat for the base module, a PC with display monitor, and a tele-rehabilitation software platform [2]. The non-motorized version employs three omni-directional wheels for smooth translation and orientation of the mobile base platform with minimal resistance to provide patients with a low-friction workspace for reach training. The system is intended for use with moderately impaired patients who have strong coupling of shoulder and elbow torques but can achieve self-initiated movements with gravitational support.

In the current (motorized) ArmAssist implementation, three low-cost servo motors have been added to provide assistive torques to each of the three omni-directional wheels. The resulting system achieves smooth rotational and translational assistive motion in accordance with the respective training task undertaken.

The aim of this paper is to present the first steps in the development of a powered mobile module in order to widen the available training strategies (and impairment levels) that can be used with the ArmAssist system. In the following section, we describe the system components of the powered mobile module. The position control scheme implemented in the module is presented in Section III and Section IV shows the results of experiments with different loading conditions and two unimpaired subjects in reach movement training. In Section V, a discussion of the test results and further challenges are presented and final conclusions are drawn in Section VI.

II. SYSTEM DESCRIPTION OF POWERED MOBILE MODULE

A. Mechanical Components

Mechanical components composing the powered mobile module are shown in Fig. 2. Among them, the wheel, actuator, forearm bar, and force sensor are described here as they are the main components that influence the movement and functionality of the powered module.

Wheel – An omni-directional mobile robot has an inherent agility, which allows simultaneous and independent motion in translation and rotation. This benefit results in the wide use of the omni-directional mobile robot in many different areas. The ArmAssist adopted omni wheels (Kornylak, FXA315) in its design to meet requirements needed to allow natural movement during arm reach training. The ArmAssist employs three omni wheels configured in an isosceles triangle on the plantar side cover plate, as shown in Fig. 2(c).

Actuator – A low-cost actuator that satisfies the torque requirements of the system was selected, and three such motors were integrated in the hardware, shown in Fig. 2(c). Table I shows the specifications of the selected motor unit along with its encoder and gear. While the motor and gear combination provide sufficient power and rotational speed required to assist movement, it may be noted that any gear ratio above 1:1 reduces system backdrivability, impairing the system’s haptic performance and ultimately, transparency to the user. It is therefore important to consider the mobility needs of the application throughout any gear selection process.

Forearm bar and 1-DOF force sensor – The forearm of the user, shown in Fig. 2(a), is positioned in a set of forearm and wrist orthoses on the forearm bar (Fig. 2(b)) which is connected to the module body by a single-axis rotational joint. The resulting design and omni-directional driving mechanism allow a patient to conduct a natural forearm movement during planar reach tasks with minimal resistance. A force sensor is integrated between the base frame and the forearm bar, measuring interaction force of the arm in the vertical direction.

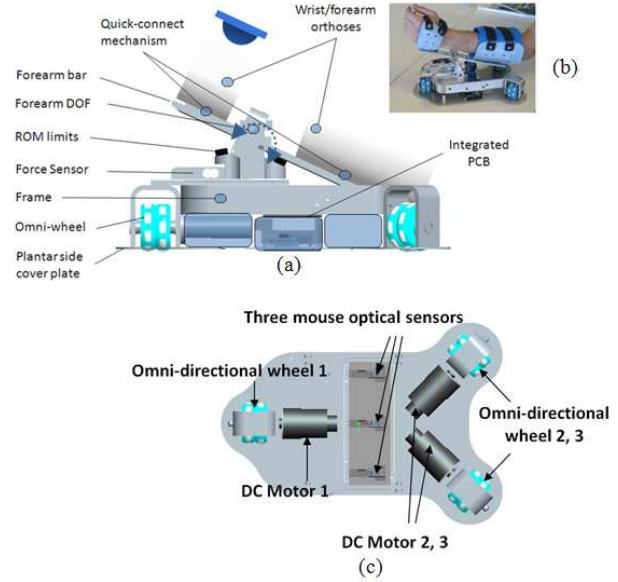
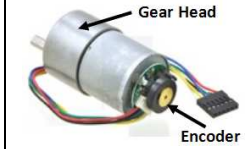


Figure 2. Structural view of the mobile module: (a) side view with mechanical components, (b) the mobile robot with a forearm, and (c) top view of plantar side cover plate with three omni-directional wheels, motors, and mouse optical sensors

TABLE I. SELECTED MOTOR SPECIFICATIONS

	Input Voltage	12V
	Maximum RPM without load	500 RPM
	Stall torque at 5A	5kg-cm
	Gear ratio	19:1
	Encoder resolution	64 CPR ^a
	Weight	212g

a. CPR: Counters per revolution

The measure and use of vertical interaction force are considered a critical factor in progressive load training.

B. Position and orientation Sensing System

To detect absolute position and orientation of the mobile base module, three mouse optical sensors (Avago Technologies, ADNS-3080) are integrated in the plantar side cover plate, illustrated in Fig. 2(c) [3]. Data from the left and right sensors are used for odometry calculations, and the third sensor takes low resolution pictures of a custom designed mat. The data and picture are transferred to the PC through a Bluetooth communication protocol and the developed sensor fusion algorithm executed in the PC calculates relatively accurate and reliable global position and orientation. The calculated values are then sent back to the module for path control. Position and orientation data are updated at 6 Hz, which is the maximum speed that ensures new information is received while data from the PC are periodically transferred at 20 Hz.

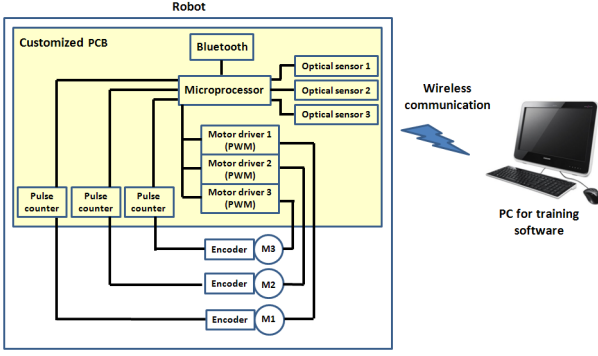


Figure 3. The customized PCB architecture

C. Customized PCB

For the sake of position and orientation sensing, a customized PCB with imbedded microprocessor was developed (Fig. 3) enabling bilateral communication between the module and PC, and motor control for up to three motors. The microprocessor (STMicroelectronics, STM32F103RB) is in charge of executing a control algorithm and managing signal flows to three motor drivers that use H-bridge circuitry and PWM signals to control the three motors.

III. CONTROL SCHEME

In this section, we present the kinematic model of the powered mobile module, the resulting position controller, and the velocity control model.

A. Kinematic model

To describe the motion of the powered mobile module, we employed two coordinate frames that facilitate the derivation of a mathematical model of a mobile robot [4]: the local module frame $\{R\}$ and the fixed world frame $\{W\}$ are shown in Fig. 4. The local module frame is a moving frame fixed on the body of the mobile module at the point of interest, which is, in this study, the center optical sensor as the position (x, y) and orientation ψ of the module is measured with respect to that point. The fixed world frame is a global non-moving reference frame in the workspace of the module.

From the mobile module geometry shown in Fig. 4, translational velocities (u, v) and rotational velocity (r) in the local module frame are given by

$$\begin{bmatrix} u \\ v \\ r \end{bmatrix} = \frac{R_w}{n} \mathbf{B}^{-1} \begin{bmatrix} \omega_{m1} \\ \omega_{m2} \\ \omega_{m3} \end{bmatrix} \quad (1)$$

where

$$\mathbf{B} = \begin{bmatrix} -1 & 0 & L_1 \\ \cos(\alpha) & -\sin(\alpha) & L_2 \cdot \cos(\beta) \\ \cos(\alpha) & \sin(\alpha) & L_2 \cdot \cos(\beta) \end{bmatrix},$$

R_w is the radius of the omni-directional wheel, n is the gear ratio of the motor, L_1 is the distance from the origin of $\{R\}$ to Wheel 1, L_2 is the distance from the origin of $\{R\}$ to Wheel 2 (or Wheel 3), α and β are angles shown in Fig. 4, and ω_{m1} , ω_{m2} ,

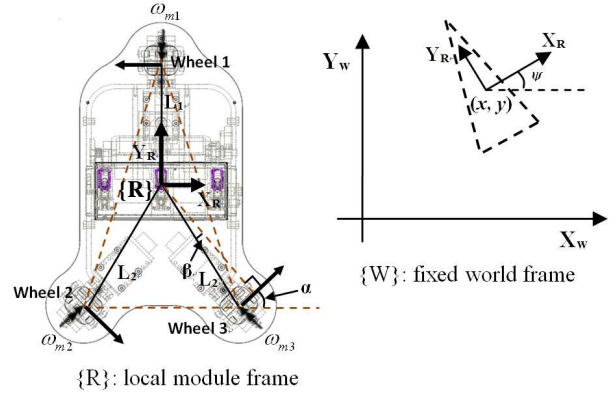


Figure 4. Geometry of the mobile module and coordinate frames

ω_{m3} are shaft velocities of the three motors. In the current design, $L_1 = 130 \text{ mm}$, $L_2 = 153 \text{ mm}$, $\alpha = 45^\circ$, and $\beta = 12^\circ$. Finally the kinematics of the module is obtained by a coordinate transformation from the local module frame to the fixed world frame

$$\begin{bmatrix} \dot{x} \\ \dot{y} \\ \dot{\psi} \end{bmatrix} = \mathbf{\Gamma} \begin{bmatrix} u \\ v \\ r \end{bmatrix} \quad (2)$$

where

$$\mathbf{\Gamma} = \begin{bmatrix} \cos(\psi) & -\sin(\psi) & 0 \\ \sin(\psi) & \cos(\psi) & 0 \\ 0 & 0 & 1 \end{bmatrix}.$$

Remark: In general, the local frame for a mobile robot is fixed at the center of gravity (COG) of the robot in order to minimize an inertia moment effect during robot rotation [4]. In this study, we selected a location of the center optical sensor as the origin of the local frame because it reduces the number of equations that are needed to calculate the module position and orientation. Since we thought that knowing the COG of the module would be helpful to understand the system and it would be required for dynamical model derivation, we roughly estimated the COG of the module using a pressure mat. The module was placed on a pressure mat and a relative pressure under each wheel was recorded in three trials. Through numerical calculation using the pressure values measured, it was found that COG of the module is located about 27 mm posterior to the center optical sensor (i.e., below the sensor in the orientation depicted in Fig. 4), the central sensor being the origin of the local module frame $\{R\}$.

B. Position Controller Architecture

A controller for path tracking was formulated based on the kinematical model derived above. It has two control loops, as shown in Fig. 5: an outer loop and an inner loop. The outer loop is a feedback PI control loop with feedforward terms that generate three motor rotational velocities $(\omega_{r1}, \omega_{r2}, \omega_{r3})$ in order to minimize the error between the desired and actual paths. The inner loop is a velocity control loop which plays a

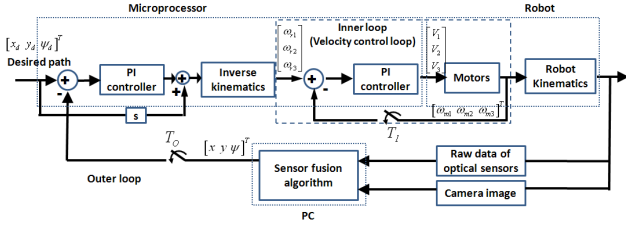


Figure 5. Controller architecture

role in producing three motor voltages (V_1 , V_2 , V_3) such that real motor rotational velocities become equal to those obtained from the outer loop. Since the control algorithms were discretely implemented in the microprocessor, all formulations are expressed in the discrete-time form such as $f(k)$, where k denotes the time at the k th sampling instance, i.e., $t = k \cdot T_c$ where T_c is a sampling frequency of the control system.

The tracking error vector is defined by

$$\mathbf{e}(k) = [x_d(k) \ y_d(k) \ \psi_d(k)]^T - [x(k) \ y(k) \ \psi(k)]^T,$$

where x_d and y_d denote the x and y coordinates of a desired path (or point), and ψ_d the desired rotation angle of the desired path in the fixed world frame $\{W\}$. Using the relationship (2) and PI controller form with feedforward terms for desired velocities of x_d , y_d , and ψ_d , the translational and rotational velocity profiles (u_r, v_r, r_r) in the local module frame $\{R\}$, which drive the module to track the desired path, are designated by

$$\begin{bmatrix} u_r(k) \\ v_r(k) \\ r_r(k) \end{bmatrix} = \mathbf{\Gamma}^{-1} \begin{bmatrix} \dot{x}_d \\ \dot{y}_d \\ \dot{\psi}_d \end{bmatrix} + \mathbf{K}_{OP} \mathbf{e}(k) + \mathbf{K}_{OI} \sum_{i=1}^k \mathbf{e}(i) \cdot T_o, \quad (3)$$

where \mathbf{K}_{OP} and \mathbf{K}_{OI} denote 3x3 diagonal constant proportional and integral gain matrices for the outer loop respectively, and T_o the sampling frequency of the outer loop. Note that T_o is set to 6 Hz, which is the frequency at which the module is able to read new updated data.

Substituting (3) into (1) and rearranging the equation with respect to the rotational velocities of the three motors (ω_{r1} , ω_{r2} , ω_{r3}), we have

$$\begin{bmatrix} \omega_{r1}(k) \\ \omega_{r2}(k) \\ \omega_{r3}(k) \end{bmatrix} = \frac{n}{R_w} \mathbf{B} \begin{bmatrix} u_r(k) \\ v_r(k) \\ r_r(k) \end{bmatrix} = \frac{n}{R_w} \mathbf{B} \cdot \mathbf{\Gamma}^{-1} \left([\dot{x}_d \ \dot{y}_d \ \dot{\psi}_d]^T + \mathbf{K}_{OP} \mathbf{e}(k) + \mathbf{K}_{OI} \sum_{i=1}^k \mathbf{e}(i) \cdot T_o \right) \quad (4)$$

Finally, the input voltages (V_1 , V_2 , V_3) for the motors in the inner loop are calculated by

$$\begin{bmatrix} V_1(k) \\ V_2(k) \\ V_3(k) \end{bmatrix} = \mathbf{K}_{IP} \mathbf{e}_\omega(k) + \mathbf{K}_{II} \sum_{i=1}^k \mathbf{e}_\omega(i) \cdot T_i \quad (5)$$

where

$$\mathbf{e}_\omega(k) = [\omega_{r1}(k) \ \omega_{r2}(k) \ \omega_{r3}(k)]^T - [\omega_{m1}(k) \ \omega_{m2}(k) \ \omega_{m3}(k)]^T,$$

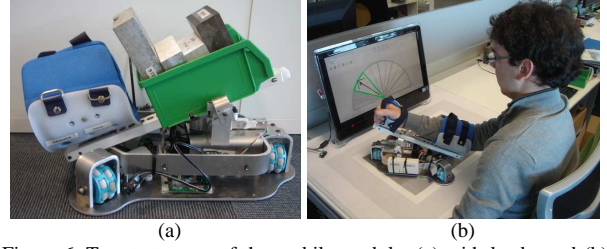


Figure 6. Two test cases of the mobile module: (a) with loads, and (b) interacting with an unimpaired subject

ω_{m1} , ω_{m2} , ω_{m3} denote real rotational velocities of three motors, \mathbf{K}_{IP} and \mathbf{K}_{II} are 3x3 diagonal constant proportional and integral gain matrices for the inner loop respectively, and T_i is the sampling frequency of the inner loop, which is 200 Hz. Rotational velocity of the motor (e.g. ω_{m1}) is obtained by performing numerical operations on the encoder signal.

IV. TEST RESULTS

The powered mobile module was tested in two different cases: 1) with five different static loading levels (the module itself, 1 kg, 2 kg, 3 kg, and 4 kg loads added), and 2) with two unimpaired subjects (Fig. 6). According to the mass distribution data of the human body [5], the weight of an arm is approximately 5% of the total body weight, meaning roughly 4 kg can be considered the maximum weight of an 80 kg person's arm. While the first test aims at evaluating the module performance under load variations, the second one is to explore the module behavior under not only load variations but also different configuration of the arm. In this section, first we present the desired path used for the test and then show test results of the developed control scheme in both cases.

A. Desired Path Selection

The tele-rehabilitation software used with the ArmAssist system provides various training and assessment programs [2]. Among them, we chose a game for assessing a user's control of vertical arm support during arm reach movements. Fig. 7 shows the desired path, specified by the game, which consists of six sets of arm reach and return motions, resulting in a shape similar to a 'star'. In the tests, the mobile module moves sequentially between the numbered locations starting from point 1 and following the straight line path connecting points 1

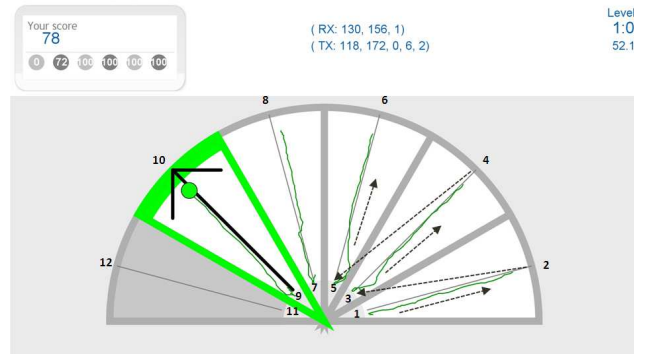


Figure 7. Selected desired path in the reaching movement game. The path is composed of six sets of coupled reaching and return motions.

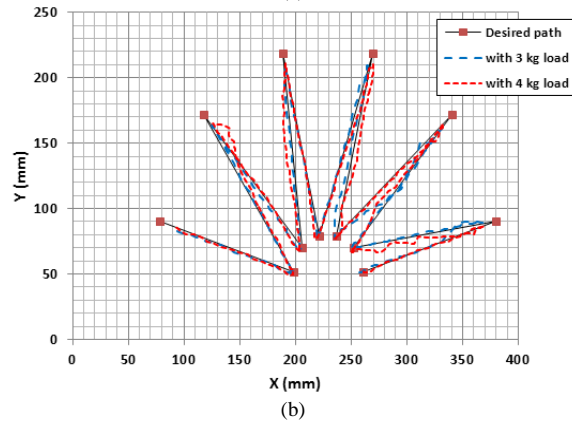
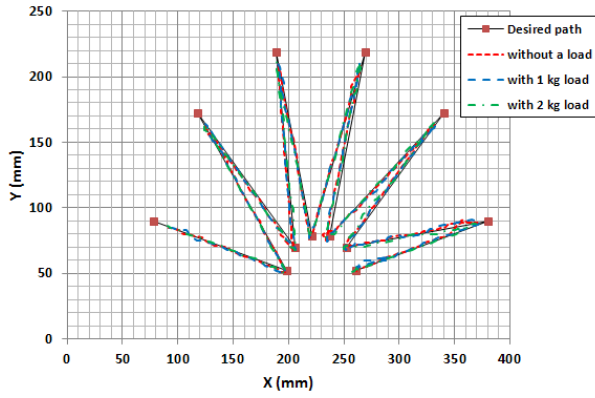


Figure 8. Actual paths of the mobile module with load: (a) 0 kg, 1 kg, and 2 kg load, and (b) 3 kg, and 4 kg load.

and 2. The module then returns to the central space at point 3 to repeat the exercise from points 3 to 4. The pattern of movement is repeated until the module reaches point 12. In both reach and return motions, the time to reach the subsequent point is set to 6 second, making the average speed of the module during tests about 20 mm/sec.

For a smooth motion, a fifth order polynomial is used to interpolate a line between the two points in both X and Y directions under the constraint that velocity and acceleration at the points are zero [6]. The resulting path makes the module depart and arrive smoothly, preventing abrupt changes of the movement speed or direction. The interpolation is carried out when the module switches path segment, from reach to return motion, and vice versa in order to move to the next target point. Note that while the developed control scheme deals with both position and orientation control of the module, in the tests, only position was taken into account in the path information because the objective of the selected reach training game was to follow the line between two points (indicated by the large black arrow in Fig. 7) regardless of the orientation.

B. Control results in five different load conditions

PI gains for the inner and outer loop were tuned to minimize tracking error with the pre-defined path. Controlled results using the gains are shown in Fig. 8. Root mean square (RMS) of the tracking error over the movement with respect to the load level is presented in Table II. The figure and table demonstrate that the error size is similar under 0, 1, and 2 kg

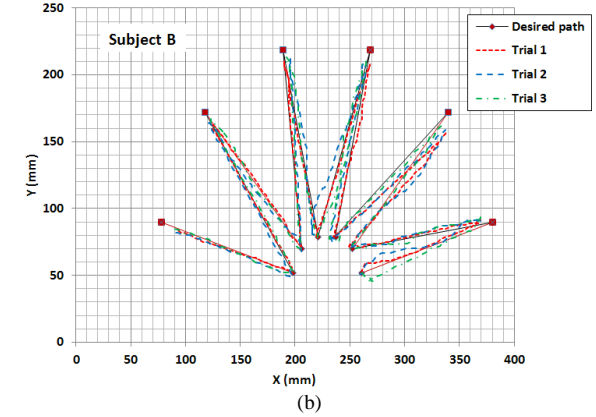
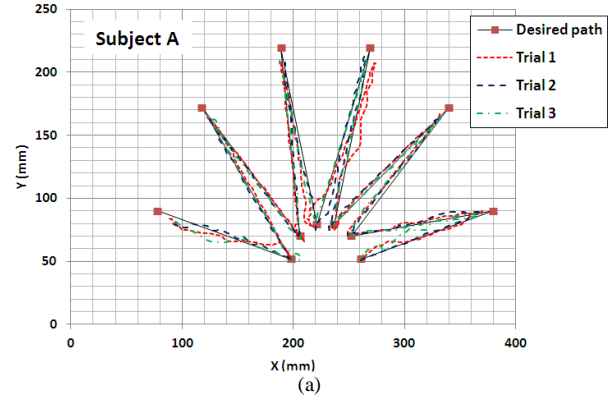


Figure 9. Actual paths of the mobile module interacting with the arm of two unimpaired subjects: (a) Subject A and (b) Subject B

load conditions while it increases proportionally to the weight in 3 kg and 4 kg load conditions.

TABLE II. RMS OF TRACKING ERROR WITH RESPECT TO THE LOAD

Load (kg)	0	1	2	3	4
RMS (mm)	4.7	4.7	4.6	6.0	11.1

C. Control results in interaction with unimpaired subjects

The aim of these tests is to explore the module behavior and performance when driving a user arm along the desired path. Two subjects participated in the test and their physical data are shown in Table III.

TABLE III. PHYSICAL DATA ON UNIMPAIRED SUBJECTS

Subject	Gender	Weight (kg)	Height (cm)
A	M	69	170
B	M	84	190

Before starting the test, subjects were asked three things: 1) to keep the shoulder at a fixed position to prevent excessive trunk movement during the test, 2) to close both eyes to not see the module path, and 3) to leave the arm on the module as natural and comfortable as possible and not make reactive force either with or against the movement of the module. The second request is to minimize subjects from subconsciously following the path while the third is to eliminate disturbances apart from the arm weight effect which varies with the kinematic configuration of the arm. Test results using the same controller and gains as in the first test are shown in Fig. 9 and average

RMS errors of 3 trials with Subject A and B are 8.3 mm and 8.4 mm respectively. From the result it can be found that the tracking performance lies between those obtained under 3 kg and 4 kg load conditions, indicating the performance of the module seems to be acceptable for training purpose with subjects.

V. DISCUSSION

A. Test results

While the module has shown an acceptable tracking performance in the pilot study, there are still several aspects that call for further investigation. First, the conditions adopted in the tests with subjects are very limited. Interaction with a patient is more complicated than with healthy users, so further testing and evaluation of the module should be performed under real conditions such as high or low muscle tone and coupling of torques between the shoulder and elbow. During tests, subjects commented that they experienced discomfort during some movements of the trajectory. We observed that it resulted from incorrect starting postures of the arm. Since the orientation of the module was not controlled, the module had a tendency to keep the starting orientation and did not actively assist the user in maintaining natural arm orientations. As a result, depending on the starting orientation, some reach movements could produce movements near the range of motion limits of the shoulder, producing higher levels of resistance from the subject. The larger deviations of Subject 1, Trial 1 (Fig. 9(a)) resulted from such instances of inadequate orientation. This finding demonstrates the importance of incorporating orientation control in the powered module in accordance with the level of arm impairment. In addition, it was observed that posture of the trunk and sitting position also should be taken into account such that the module workspace remains within the workspace of the arm in order to minimize undesired sources of discomfort.

B. Challenges

Unlike high-cost robotic devices for upper limb rehabilitation, the developed powered module does not include a multi-axis force sensor measuring forces in the driving directions. Rather, a single-axis force sensor measures loading conditions in the vertical direction. This is likely to limit force based control strategies such as impedance control, which have been widely adopted in robot-mediated therapy while their effectiveness is still under study [7]. However, control strategies designed with position information can be implemented in our powered module, including for example, automated movement guidance (used in this paper), error-amplification, and resistive training, etc. [8]. Acknowledging that a mobile base system shares some of the benefits of both end-effector and exoskeleton solution designs, the selection of the most appropriate control strategies for mobile base systems is a challenging topic to be addressed.

From the control point of view, while the module reveals an acceptable level of tracking performance, there are still several ways it can be improved. One of them is to increase the sampling frequency of the outer loop (T_o), which strongly

affects the control performance. The current maximum sampling frequency is 6 Hz and it is limited by the filtering of data from PC to ensure that the module reads the updated data, resulting in the increase in tracking error under the load conditions with the mass higher than 2 kg. The frequency can be increased by directly processing a camera image in a microprocessor with higher computation power. Replacing the velocity control in the inner loop with current control can also lead to improved performance. The low resolution of the encoder attached to the motor produces a 5 RPM (revolutions per minute) resolution in angular velocity, resulting in poor control performance when the module moves slowly. Though a high resolution encoder can be a solution, implementing the current loop has an advantage because an encoder is no longer necessary.

VI. CONCLUSION

In this paper, the first developmental results of a powered mobile module for the ArmAssist home-based telerehabilitation system have been presented. Three DC motors, considering cost efficiency, were selected and integrated in the mobile module. A position controller composed of two loops, an inner and outer loop, using a PI control structure was developed and tested in experiments with different loads and two unimpaired subjects in pre-defined path following tasks. Test results indicate that the module is capable of assisting arm movements within an acceptable tracking error range in healthy subjects. Further tests under more realistic conditions to better reflect interactions with a range of post-stroke impairments are required for clinical engagement of the module. Moreover, implementing and testing other control strategies developed for robot assisted training will be a future topic of interest.

REFERENCES

- [1] J. C. Perry, H. Zabaleta, A. Belloso, and T. Keller, "ARMassist: A low-cost device for telerehabilitation of post-stroke arm deficits," World Congress on Medical Physics and Biomedical Engineering, 2009, Munich, Germany, IFMBE Proceedings, 2009, vol. 25(9), pp. 64-67.
- [2] J. C. Perry, H. Zabaleta, A. Belloso, C. Rodriguez-de-Pablo, F. I. Cavallaro, and T. Keller, "ArmAssist: development of a functional prototype for at home telerehabilitation of post-stroke arm impairment," Conf. on Biomed. Robo. and Biomecha. (BioRob) 2012, pp. 1561-1566.
- [3] H. Zabaleta, D. Valencia, J. Perry, J. Veneman, and T. Keller, "Absolute position calculator for a desktop mobile robot based on three optical mouse sensors," Conf Proc IEEE Eng Med Biol Soc (EMBC) 2011, pp. 2069-2072.
- [4] Y. Liu, J. J. Zhu, R. L. Williams II, and J. Wu, "Omni-directional mobile robot controller based on the trajectory linearization," Robotics and Autonomous Systems, vol. 56, pp. 461-479, 2008.
- [5] D.A. Winter, Biomechanics and Motor Control of Human Movement, John Wiley & Sons, 3rd edition, 2005.
- [6] J. J. Craig, Introduction to Robotics, Addison-Wesly Publishing Company, 2nd edition, 1989.
- [7] L. E. Kahn, P. S. Lum, W. Z. Rymer, and D. J. Reinkensmeyer, "Robot-assisted movement training for the stroke-impaired arm: Does it matter what the robot does?," Journal of Rehabilitation Research & Development (JRRD), vol. 43(5), pp. 619-630, 2006.
- [8] L. Marchal-Crespo, and D. J. Reinkensmeyer, "Review of control strategies for robotic movement training after neurologic injury," Journal of NeuroEngineering and Rehabilitation, vol. 6(20), 2009.